Nuclear Instruments and Methods in Physics Research A 639 (2011) 155–157

Contents lists available at ScienceDirect

Nuclear Instruments and Methods in Physics Research A

journal homepage: www.elsevier.com/locate/nima

Comparison of secondary electron emission simulation to experiment ☆

Z. Insepov [a,*], V. Ivanov [b], S.J. Jokela [a], I. Veryovkin [a], A. Zinovev [a], H. Frisch [a]

[a] Argonne National Laboratory, 9700 S. Cass Avenue, Argonne, IL 60439, USA
[b] Muons, Inc., 552 N. Batavia Avenue, Batavia, IL 60610, USA

ARTICLE INFO

Available online 10 November 2010

Keywords:
Secondary electron emission
Monte Carlo simulation
Gold

ABSTRACT

Monte Carlo simulation, empirical theories, and close comparison to experiment were used to parameterize the secondary electron emission (SEE) yields of several highly emissive materials for microchannel plates. In addition, a detailed experiment and analysis of gold were carried out at Argonne National Laboratory. The simulation results will be used in the selection of emissive and resistive materials for deposition and characterization experiments that will be conducted by a large-area fast detector project at Argonne.

1. Introduction

Theoretical models of secondary electron emission (SEE) yields for highly emissive materials are important for the development of particle detectors for high-energy physics, such as Cherenkov, neutrino, and astroparticle detectors, as well as for the development of scanning electron microscopy [1–15].

In this work, a parameterized set of the SEE-yield dependencies on two variables, the primary electron energy (E_{PE}) and the angle of incident electrons (θ), was obtained by Monte Carlo simulation and the simulation results are compared to the experimental data for several highly emissive materials of interest for the development of large-area microchannel plates (MCPs) fast detectors.[1]

The calculations were verified with experimental data for gold as a reference material, specifically measured for the large-area fast detector project. The calculated yields will be used mainly as input files for macroscopic gain and transient time calculation codes for computing electron trajectories inside MCPs of various types, such as chevron and funnel. Feedback from the gain code will then be used to improve the materials data and will stimulate further search for the best MCP emissive materials.

2. Secondary electron emission yields

Several semi-empirical theories have been developed regarding secondary electron emission yield [7–13]. These theories are helpful in calibrating the Monte Carlo (MC) simulations, which are the main tool for obtaining the SEE yields for various materials at different energies and incident angles of primary electrons. Specifically, if no reliable theoretical or experimental data exists for the parameters of secondary emission yields, such data can be obtained from the MC simulations and then can be used to quantify the SEE yields for new materials using the empirical laws. An extensive analysis has been done by Lin and Joy [8], who obtained a universal law for 44 elements with $Z=3-83$.

Several researchers have developed Monte Carlo codes based on the above theory that are applicable to low-energy SEE-yield calculations [3,4,7–9]. The Rutherford cross-section for elastic electron scattering of low-E electrons and high-Z materials was replaced by Mott's cross-section, which was tabulated for the electron energies in the range of 1–100 keV [3]. The inelastic energy loss of electrons is usually approximated by Bethe's equation, which was improved by Seiler [12] for low-energy electrons. Two important simulation parameters are used in the Monte Carlo model. One is ε, the average energy for producing secondary electron, and the other is the escape length λ. These two parameters have a significant impact on the simulation results.

We used $\varepsilon=20$ eV for Al_2O_3 [10]. The escape length λ of insulators can be relatively large compared to that of metal surfaces, a direct effect of the small absorption coefficient of low-energy electrons in insulators because of the large energy band gap (e.g., $E_g=8$ eV in Al_2O_3). Kanaya et al. [11] proposed a theoretical model for calculating the escape length for a range of insulators and alkaline materials. Based on this analysis, the escape length can be chosen as $\lambda=60$ Å for Al_2O_3. This value was also suggested by Joy [10].

☆The submitted manuscript has been created by UChicago Argonne, LLC, Operator of Argonne National Laboratory ("Argonne"). Argonne, a U.S. Department of Energy Office of Science Laboratory, is operated under Contract no. DE-AC02-06CH11357. The U.S. Government retains for itself, and others acting on its behalf, a paid-up nonexclusive, irrevocable worldwide license in said article to reproduce, prepare derivative works, distribute copies to the public, and perform publicly and display publicly, by or on behalf of the Government.

* Corresponding author. Tel./fax: +1 630 252 5049.
E-mail address: insepov@anl.gov (Z. Insepov).

[1] https://hepblog.uchicago.edu/cdf/cdf2/

0168-9002/$ - see front matter © 2010 Elsevier B.V. All rights reserved.
doi:10.1016/j.nima.2010.10.048

Table 1
Material parameters.

Material	ε (eV)	λ (Å)
Al_2O_3	20 [9]	60 [10]
MgO	20 [11]	120 [11]
ZnO	125 [11]	20–40 [this work]
Gold	40 [8]	7 [8]

The simulation results for electron energies above ~200 eV were obtained using Monte Carlo codes developed in [3,4,7–9]. A detailed explanation of the algorithm used in these codes can be found in [3,7].

The Rutherford cross-section is used to calculate the mean free path of the electron and the directions of the scattered electron. The inelastic energy loss is calculated according the Bethe stopping power equation modified at low energies. The number of the secondary electrons is calculated in a simple Salow–Dekker approximation and their probability to escape to the surface is chosen to be an exponential function of the distance to the surface.[7]. For electrons with energies below ~200 eV, the inelastic energy loss was modified according to the algorithm proposed by Joy [9]. For electron energies below 50 eV, we used the "universal law of SEE yield" given in [8].

The escape length of ZnO was used as an adjustable parameter. The following material parameters were used: λ was varied between 40 Å for low-energy and 20 Å for high-energy regions, according to a suggestion by Joy [9], and ε was set to 125 eV [11]. These parameters are listed in Table 1.

3. Comparison with experiment

Since the charging of highly resistive ceramics makes it difficult to obtain correct SEE-yield results, it is important to compare simulations with the experimental data obtained with a pulsed technique by Dowson [16]. Fig. 1 shows our comparison of the emission rates obtained by simulation with the experimental measurements for various thin film structures of Al_2O_3. Our result shows close agreement between experiment [16] and our simulations.

Monte Carlo simulations were also conducted for the SEE yields of ZnO samples, and the results of our simulations were compared with the experimental results of Gornyi [17]. Also this material is not highly emissive, it was used for increasing conductivity of the mixture Al_2O_3 and ZnO. The agreement between the simulated and measured data is close at the maximum of SEE yield but less comparable at the low-energy end.

Our Monte Carlo results were also compared with MgO data measured in [18–20]. We have obtained good comparison with the result measured by Dekker [20].

A detailed study of SEE was carried out for gold, since this material was chosen as a reference for our secondary electron emission experiments.

Our experimental setup used the electron gun from a low-energy electron diffraction system as an electron source of fixed energy, 850 eV, for this experiment. The kinetic energy of the electrons was varied by applying a negative potential to the sample using a Keithley Source Meter, which also sampled the electrical current flow. The initial beam current, I_{beam}, was sampled by applying a positive 1100 V bias to the sample, preventing all secondary electrons from escaping. We then varied the sample voltage from −850 to 0 V in 1 V increments, measuring the current flow at every point. The gain, γ, was then calculated using the following equation:

$$\gamma = \frac{I_{collector}}{I_{beam}} = 1 - \frac{I_{sample}}{I_{beam}} \quad (1)$$

where instead of using an external collector to collect the secondary electrons, we simply measure the current flowing from the voltage source used to bias the sample, I_{sample}.

This system is included in an ultra-high vacuum chamber (4×10^{-10} Torr) along with a 5 keV Ar-ion source for sputter cleaning and an X-ray photoelectron spectrometer that uses a Mg K-alpha X-ray source (1253 eV) and a hemispherical electron energy analyzer (HA100 from VSW Scientific Instruments). The X-ray beam is neither collimated nor passed through a monochromator. However, the X-ray emission is narrow enough to obtain compositional information as well as some chemical information from samples. This system also includes a helium UV source for use in ultraviolet photoelectron spectroscopy, which will be used in the future to better relate band structure with surface composition and how they tie into the secondary electron emission of a broad range of materials.

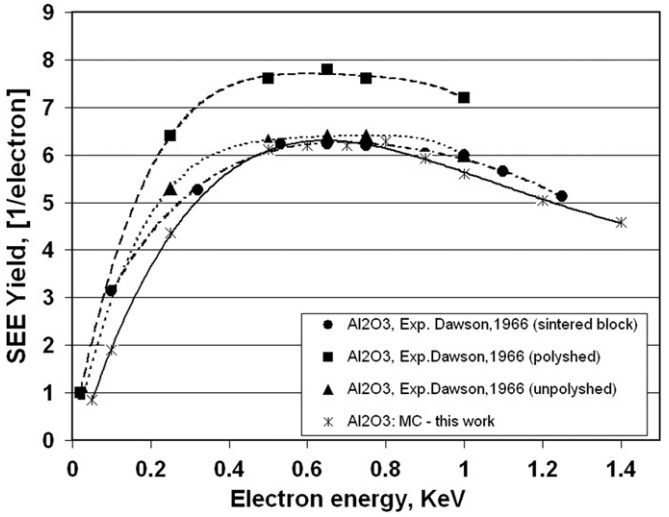

Fig. 1. Comparison of our results calculated by Monte Carlo method for Al_2O_3 with experimental data obtained in [16] for polished (squares and dashed line), unpolished (triangles and dotted line), and sintered surface (circles and dash-dotted) curves and symbols. Our simulation is shown as stars symbols and fitted by solid curve.

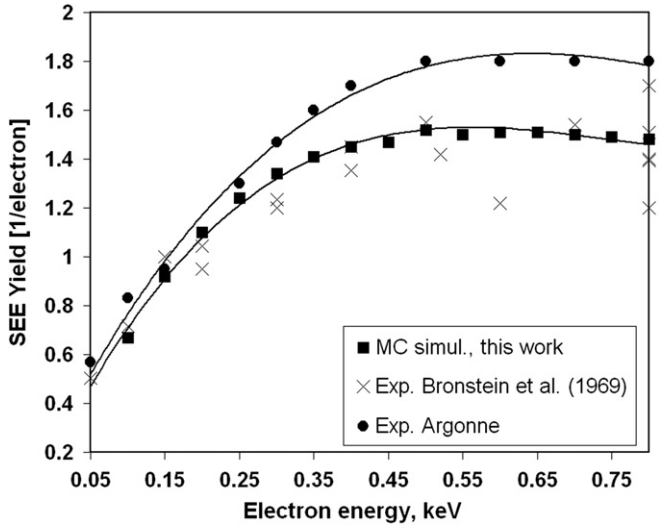

Fig. 2. Secondary electron yield for gold foil measured in this work after 30 min Ar-ion sputter cleaning (solid circles) and in experiment [21] (crosses) compared with our calculations (solid squares).

Our analysis of gold showed a strong correlation between surface composition/cleanliness and secondary electron emission. The gold foil sample used in this study had been stored on a shelf and had an unknown history. Sample composition and secondary electron yield as a function of incident electron energy were measured before and after 5 keV Ar^+ sputter cleaning. Before Ar-ion cleaning, we observed a strong carbon and oxygen contamination, most likely from surface contamination accumulated during the storage of the sample.

It is suspected that the surface contamination provides an extra barrier for secondaries escaping the surface. This layer may also provide some secondary electrons as the primary electrons pass through.

After Ar-ion cleaning, we see the near-elimination of carbon and oxygen contamination. There also appears to be an increase in Si from an unknown source. It is possible that this Si is an impurity in the gold foil. We also see an increase in secondary electron yield (Fig. 2). This shows that even a small amount of contamination on the surface greatly affects the secondary yield of a sample.

Acknowledgments

We thank D. Joy and P. Hovington for sharing their codes and giving valuable suggestions for the simulation parameters.

This work was supported in part by the Office of Advanced Scientific Computing Research, Office of Science, U.S. Department of Energy, under Contract DE-AC02-06CH11357.

References

[1] E. Nappi, Nucl. Instr. and Meth. A 604 (2009) 190.
[2] S.M. Bradbury, R. Mirzoyan, J. Gebauer, E. Feigl, E. Lorenz, Nucl. Instr. and Meth. A387 (1997) 45.
[3] L. Reimer, D. Stelter, Scanning 8 (1986) 265.
[4] S. Ishimura, M. Aramata, R. Shimizu, J. Appl. Phys. 51 (1980) 2853.
[5] D.R. Beaulieu, D. Gorelikov, P. de Rouffignac, K. Saadatmand, K. Stenton, N. Sullivan, A.S. Tremsin, Novel microchannel plate device fabricated with atomic layer deposition, in: Proceedings of the AVS Topical Conference on Atomic Layer Deposition, ALD 2009, Monterey, CA, July 19–22, 2009.
[6] J.A. Anderson1, K. Byrum1, G. Drake1, C. Ertley, H. Frisch, J.-F. Genat, E. May, D. Salek, F. Tang, New developments in fast-sampling analog readout of MCP based large-area picosecond time-of-flight detectors, IEEE-MIC 2008, ID-2973.
[7] D.C. Joy, Monte Carlo Modeling for Electron Microscopy and Microanalysis, Oxford University Press, 1995.
[8] Y. Lin, D.C. Joy, Surf. Interface Anal. 37 (2005) 895.
[9] D.C. Joy, J. Microsc. 147 (1987) 51.
[10] D.C. Joy, Private communication, 2009.
[11] K. Kanaya, S. Ono, F. Ishigaki, J. Phys. D 11 (1978) 2425.
[12] H. Seiler, J. Appl. Phys. 54 (1983) R1.
[13] J.R. Young, Phys. Rev. 103 (1956) 292.
[14] R.O. Lane, D.I. Zaffarano, Phys. Rev. 94 (1954) 960–964.
[15] K. Ohya, I. Mori, J. Phys. Soc. Jpn. 59 (1990) 1506.
[16] P.H. Dawson, J. Appl. Phys. 37 (1966) 3644.
[17] N.B. Gornyi, J. Exp. Theor. Phys. 26 (1954) 88 in Russian.
[18] N.R. Whetten, A.B. Laponsky, J. Appl. Phys. 28 (1957) 515.
[19] Y. Ushio, T. Banno, N. Matuda, Y. Saito, S. Baba, A. Kinbara, Thin Solid Films 167 (1988) 299.
[20] A.J. Dekker, Secondary electron emission, in: F Seitz, D Turnbull, H Ehrenreich (Eds.), Solid State Phys., vol. 6, Academic Press, New York1958, pp. 251–311.
[21] I.M. Bronstein, B.S. Fraiman, Vtorichnaya Elektronnaya Emissiya, 1969 (in Russian).